**doi:10.1016/j.ijrobp.2007.01.034**

# CHANGES IN CEREBRAL CORTEX OF CHILDREN TREATED FOR MEDULLOBLASTOMA

ARTHUR K. LIU, M.D., PH.D.,* KAREN J. MARCUS, M.D.,[†‡§] BRUCE FISCHL, PH.D.,[∥¶]
P. ELLEN GRANT, M.D.,[#] TINA YOUNG POUSSAINT, M.D.,** MICHAEL J. RIVKIN, M.D.,[††]
PETER DAVIS, B.S.,[††] NANCY J. TARBELL, M.D.,[‡‡] AND TORUNN I. YOCK, M.D.[‡‡]

*Harvard Combined Radiation Oncology Program, Harvard Medical School, Boston, MA; [†]Department of Radiation Oncology, Children's Hospital Boston, Harvard Medical School, Boston, MA; [‡]Department of Radiation Oncology, Dana Farber Cancer Institute, Harvard Medical School, Boston, MA; [§]Department of Radiation Oncology, Brigham and Women's Hospital, Harvard Medical School, Boston, MA; [∥]Athinoula A. Martinos Center, Massachusetts General Hospital, Harvard Medical School, Charlestown, MA; [¶]Department of Computer Science and Artificial Intelligence Laboratory, Massachusetts Institute of Technology, Division of Health Sciences and Technology, Cambridge, MA; [#]Department of Radiology, Massachusetts General Hospital, Harvard Medical School, Boston, MA; **Department of Radiology, Children's Hospital Boston, Harvard Medical School, Boston, MA; [††]Departments of Neurology, Psychiatry, and Radiology, Children's Hospital Boston, Harvard Medical School, Boston, MA; [‡‡]Department of Radiation Oncology, Massachusetts General Hospital, Harvard Medical School, Boston, MA

**Purpose:** Children with medulloblastoma undergo surgery, radiotherapy, and chemotherapy. After treatment, these children have numerous structural abnormalities. Using high-resolution magnetic resonance imaging, we measured the thickness of the cerebral cortex in a group of medulloblastoma patients and a group of normally developing children.
**Methods and Materials:** We obtained magnetic resonance imaging scans and measured the cortical thickness in 9 children after treatment of medulloblastoma. The measurements from these children were compared with the measurements from age- and gender-matched normally developing children previously scanned. For additional comparison, the pattern of thickness change was compared with the cortical thickness maps from a larger group of 65 normally developing children.
**Results:** In the left hemisphere, relatively thinner cortex was found in the perirolandic region and the parieto-occipital lobe. In the right hemisphere, relatively thinner cortex was found in the parietal lobe, posterior superior temporal gyrus, and lateral temporal lobe. These regions of cortical thinning overlapped with the regions of cortex that undergo normal age-related thinning.
**Conclusion:** The spatial distribution of cortical thinning suggested that the areas of cortex that are undergoing development are more sensitive to the effects of treatment of medulloblastoma. Such quantitative methods may improve our understanding of the biologic effects that treatment has on the cerebral development and their neuropsychological implications. © 2007 Elsevier Inc.

Medulloblastoma, Cortical thickness, Magnetic resonance imaging.

## INTRODUCTION

Children with medulloblastoma are typically treated with a combination of surgery, radiotherapy, and chemotherapy. These children often develop late neurocognitive sequelae, such as significant decreases in intellectual function (1–10), poor academic performance (6, 11, 12), and deficits in attention (4, 11, 13), memory (4, 11), verbal fluency (4, 5, 7, 11), and executive functioning (11).

These side effects could be related to a variety of structural abnormalities in the brain that have been found after such intensive therapy (14–19). A number of groups have made quantitative volumetric measurements of gray and white matter using magnetic resonance imaging (MRI) (referred to as "quantitative MRI") in patients undergoing such intensive therapy (20–26). These studies found that the gray matter volume was unaffected by treatment but that the normal-appearing white matter was decreased in children with medulloblastoma who underwent radiotherapy compared with children with low-grade gliomas treated with surgery alone (26) or healthy children (21). The decrease in the amount of normal-appearing white matter also correlated with the craniospinal radiation dose (24). Decreased amounts of normal-appearing white matter correlated with decreases in full-scale intelligence quotient (IQ), factual knowledge, verbal thinking, nonverbal thinking, attention, and academic achievement (22, 23, 25).

These extensive neurocognitive deficits strongly suggest that the cerebral cortex, which plays an integral role in higher order cognition, is also affected by treatment of medulloblastoma. Although previous quantitative MRI studies did not find changes in the gray-matter volumes, this could have been a result of the limitations of their methods, because evaluation of the gray matter was limited to that in a single axial slice.

The purpose of our study was to use a more sensitive technique with high-resolution MRI and an automated cerebral cortical reconstruction technique (27) to compare the thickness of the cortex over the entire brain of 9 children treated for medulloblastoma with that of 9 normally developing children matched for gender and age. We hypothesized that treatment of medulloblastoma would result in abnormal gray-matter development.

## METHODS AND MATERIALS

### Subjects

This institutional review board-approved study included 9 children with medulloblastoma treated either at Massachusetts General Hospital for Children (*n* = 8) or Children's Hospital Boston (*n* = 1) between 1996 and 2005 (Table 1). Eight had standard-risk medulloblastoma and one had high-risk disease because of tumor infiltration into the brainstem and resulting subtotal resection. The average age at diagnosis was 8.9 years (range, 5.4–13.9 years). The average time from diagnosis to the MRI scan was 2.8 years (range, 1.0–8.2 years). The boost volume for 8 subjects consisted of the entire posterior fossa. For

Table 1. Patient characteristics

| Pt. No. | Risk category | Gender | Age at diagnosis (y) | CSI dose (Gy) | PF Dose (Gy) | Total PF dose (Gy) | Age at scan (y) | Age of matched control (y) | Interval from diagnosis to scan | Concurrent chemotherapy | Adjuvant chemotherapy |
|---|---|---|---|---|---|---|---|---|---|---|---|
| 1 | Standard | M | 13.9 | 23.4 | 30.6 | 54.0 | 16.6 | 16.2 | 2.8 | Vincristine | Cisplatin, lomustine, vincristine |
| 2 | Standard | F | 8.3 | 23.4 | 30.6 | 54.0 | 10.6 | 10.8 | 2.2 | Vincristine | Cisplatin, lomustine, vincristine |
| 3 | Standard | F | 5.5 | 23.4 | 30.6 | 54.0 | 7.2 | 7.3 | 1.7 | Vincristine | Cisplatin, lomustine, vincristine |
| 4 | Standard | M | 10.7 | 30.6 | 23.4 | 54.0 | 12.6 | 12.5 | 1.9 | Vincristine | Cisplatin, cytoxan, vincristine |
| 5 | High | M | 10.1 | 36.0 | 18 | 54.0 | 15.3 | 14.6 | 5.2 | Vincristine | Cisplatin, lomustine, vincristine |
| 6 | Standard | M | 5.4 | 24.0 | 30.5 | 54.5 | 13.6 | 13.6 | 8.2 | Vincristine | Cisplatin, lomustine, vincristine |
| 7 | Standard | M | 6.3 | 23.4 | 30.6 | 54.0 | 7.2 | 7 | 1.0 | Vincristine | Cisplatin, cytoxan, etoposide, vincristine |
| 8 | Standard | M | 6.3 | 23.4 | 30.6 | 54.0 | 7.4 | 7.7 | 1.1 | Vincristine | Cisplatin, cytoxan, etoposide, vincristine |
| 9 | Standard | F | 13.2 | 23.4 | 30.6 | 54.0 | 14.5 | 14.5 | 1.3 | None | Cisplatin, cytoxan, etoposide, vincristine |
| Mean | | | 8.9 | 25.7 | 28.4 | 54.1 | 11.7 | 11.6 | 2.8 | | |
| SD | | | 3.3 | 4.5 | 4.6 | 0.2 | 3.7 | 3.5 | 2.4 | | |

*Abbreviations:* Pt. No. = patient number; CSI = Craniospinal Irradiation; PF = posterior fossa; M = male; F = female.

Patient 2, the boost volume consisted of the tumor bed plus a 1.5-cm margin. During the radiotherapy planning, no specific attempt was made to minimize the dose to any brain structures, including the temporal lobes. Eight of the children received vincristine concurrently with craniospinal irradiation. All the children underwent adjuvant chemotherapy. Appropriate institutional informed consent was obtained.

The comparison group consisted of 9 normal children who had previously undergoing MRI at Children's Hospital Boston for the MRI Study of Normal Brain Development (28). The control subjects were gender matched, with age matched as closely as possible (Table 1). A nonmatched cohort of 62 scans from 56 additional normally developing children (24 boys and 32 girls; average age, 10.7 years; range, 5.0–17.7 years) was added to those of the 9 matched control patients to create a model of the effect of age on cortical thickness.

### MRI studies

A 1.5-Tesla GE MRI scanner was used for all imaging. The MRI protocol for the medulloblastoma patients varied slightly at the two institutions. Massachusetts General Hospital for Children used a high-resolution $T_1$-weighted three-dimensional spoiled gradient recalled acquisition in steady state (SPGR) sequence (echo time, 8 ms; repetition time, 32 ms, and 25° flip angle) with a 220-mm field of view, 256 × 256 matrix, and 124 1.5-mm slices. Children's Hospital Boston used a high-resolution $T_1$-weighted three-dimensional SPGR sequence (echo time, 1.4 ms; repetition time, 6 ms; and 14° flip angle) with a 250-mm field of view, 256 × 256 matrix, and 124 1.3-mm slices. All the normally developing children underwent MRI at Children's Hospital Boston using a high-resolution $T_1$-weighted three-dimensional SPGR sequence (echo time, 10 ms; repetition time, 24 ms; and 20° flip angle) with a 240-mm field of view, 256 × 256 matrix, and 124 1.2-mm slices. These MRI sequences are not typical for routine clinical scanning and thus limited the number of children available for this study.

### Cortical surface reconstruction

The automated segmentation tools used high-resolution $T_1$-weighted MRI scans. The reconstruction technique began with the segmentation of gray matter and white matter (27, 29–33) to generate the representation of the gray matter–white matter boundary. After the initial surface model had been constructed, a refinement procedure was applied to obtain an accurate representation of the gray–white interface. This surface was subsequently deformed outward to obtain an explicit representation of the gray matter–cerebrospinal fluid boundary, which we refer to as the pial surface. Smoothness constraints on the evolving surface allowed the accuracy of the surface models to exceed that of the underlying MRI data. Finally, we used a method for automatic correction of topologic defects to ensure accurate geometry and topologic relationships. The explicit construction of the gray–white surface and pial surface boundaries allowed the accurate, automated measurement of the thickness of the entire cortical sheet. This MRI-based technique provides thickness values within 0.2 mm of measurements taken from pathologic specimens (34) and has a test-retest accuracy of 0.1 mm (27).

Finally, comparison among subjects requires intersubject registration. We used an approach that includes a spherical atlas (31). The reconstructed surface of each individual subject was first mapped onto a sphere, using a maximally isometric transformation. The surfaces were then morphed to register with an average, canonical surface, guided by a combination of folding-alignment (sulcus/gyrus) and isometric-preserving forces. A unified latitude and longitude system could then be established, allowing surface-based averaging across the subjects.

Statistical maps were displayed on the average cortical surface generated from the atlas of brains used for the registration procedure. Noncortical areas on the medial aspect, such as the corpus callosum and brainstem, were masked out and excluded from analysis.

### Statistical analysis

The cortical thickness was smoothed using a circularly symmetric gaussian smoothing kernel with a full width at half-maximum of 3 cm. The smoothing kernel was applied along the cortical surface, not in three dimensions, to improve the signal/noise ratio and minimize the averaging of non-neighboring anatomic regions of the cortex. After surface-based registration among the subjects, the cortical thickness for each child treated for medulloblastoma was compared with the corresponding matched control, point by point across the entire brain using a paired $t$ test. Differences were considered significant at $p < 0.05$.

The larger cohort of normally developing children was used to estimate the effect of age on cortical thickness. To test for the effects of age on cortical thickness, the thickness at each point was
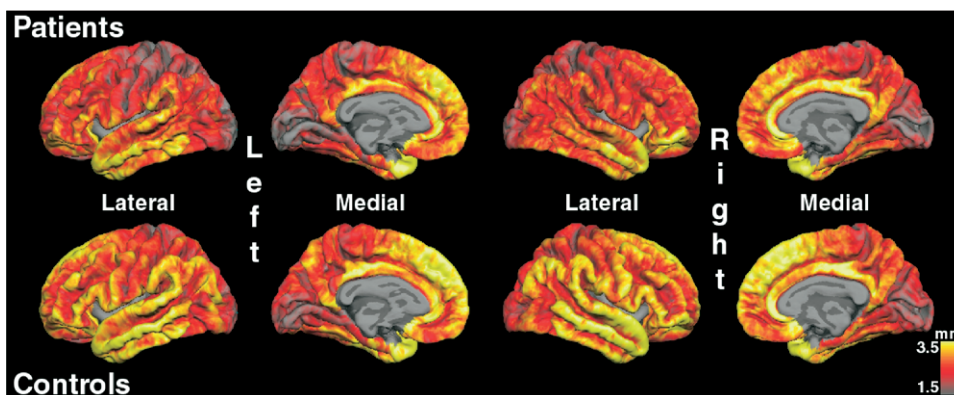


Fig. 1. Average cortical thickness maps for children treated for medulloblastoma and controls. Maps displayed on average cortical surface. Thickness of cortex represented with heat color scale, with red corresponding to cortical thickness of ≤1.5 mm and yellow corresponding to cortical thickness of ≥3.5 mm.
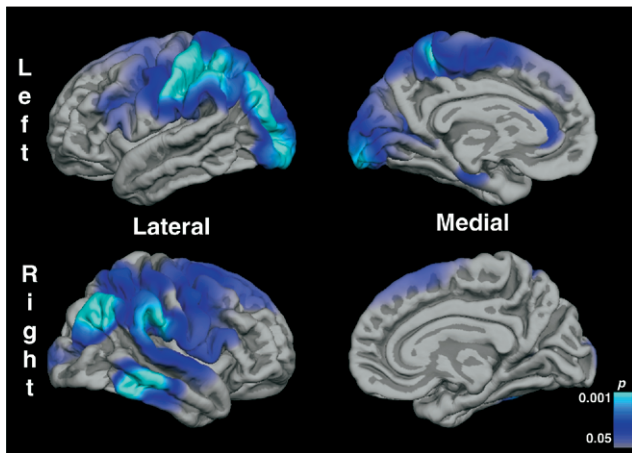
Fig. 2. Statistical maps of differences in cortical thickness between children treated for medulloblastoma and control children for left (top) and right (bottom) hemispheres. Maps displayed on average cortical surface. Maps considered significant at $p < 0.05$. Blue and cyan correspond to regions of cortex of children treated for medulloblastoma that were thinner than those of control children.



Fig. 3. Statistical map of age-dependent cortical thinning in left (Top) and right (Bottom) hemispheres of normally developing children. Maps displayed on average cortical surface. Maps considered significant at $p < 0.05$. Blue ($p < 0.05$) and cyan ($p < 10^{-6}$) correspond to regions of cortex thinner in older children.

modeled as the subject's age multiplied by a slope plus an offset. The slope and offset were estimated within the framework of a general linear model, and separate slopes and offsets were estimated for each gender. We then tested the null hypothesis that the age slope, averaged across genders, was equal to 0. Age-dependent changes were considered significant at $p < 0.05$.

## RESULTS

After spatial registration of the cortical surfaces, the average cortical thickness maps for the subjects and controls were generated (Fig. 1). In both patients and control subjects, a thinner cortex was seen posteriorly in the parietal and occipital cortex. A thicker cortex was seen anteriorly in the frontal and temporal lobes.

Maps of the areas with statistically significant differences in cortical thickness between the subjects and controls are shown in Fig. 2. All the differences reflect relative cortical thinning in the children treated for medulloblastoma. No areas were found that were thicker in the patients than in the matched controls. All regions of cortical thinning were seen bilaterally in the posterior portions of the brain. In the left hemisphere, relatively thinner cortex was found in the peri-

rolandic region and parieto-occipital lobe. In the right hemisphere, relatively thinner cortex was found in the parietal lobe, posterior superior temporal gyrus, and lateral temporal lobe. The differences in average thicknesses for the two groups for each of the above areas is given in Table 2. The differences in thickness ranged from 0.23 to 0.39 mm. However, this small, but statistically significant, difference was less than the voxel size and could not be detected visually.

The statistical maps of cortical changes with increasing age for the 65 normally developing children are shown in Fig. 3. Large distributed regions of the cortex in the frontal, parietal, occipital, and posterior temporal lobes become thinner with increasing age; none became thicker with increasing age. The cortex in the posterior frontal and anterior temporal lobes did not significantly change with age.

The areas of relative cortical thinning in the medulloblastoma patients (outlined in white at a statistical threshold of $p < 0.001$) were compared with the map of age-related thinning in normal children in Fig. 4. All the areas of relative cortical thinning were found in the regions of cortex that undergo normal age-related cortical thinning.

Table 2. Differences in average thickness for both groups

| Location | Patient average | Patient SD | Control average | Control SD | Difference |
|---|---|---|---|---|---|
| Left parieto-occipital | 2.11 | 0.19 | 2.50 | 0.10 | −0.39 |
| Left perirolandic | 1.99 | 0.22 | 2.37 | 0.10 | −0.38 |
| Right parietal | 2.40 | 0.17 | 2.70 | 0.11 | −0.30 |
| Right posterior superior temporal gyrus | 2.48 | 0.20 | 2.84 | 0.15 | −0.37 |
| Right temporal | 2.80 | 0.12 | 3.03 | 0.14 | −0.23 |

*Abbreviation:* SD = standard deviation.
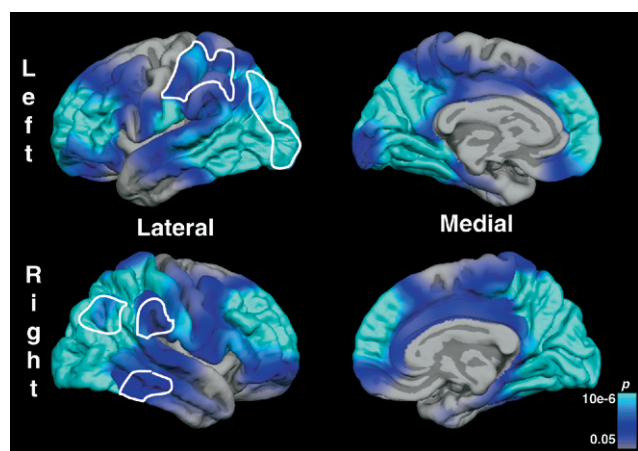
Fig. 4. Areas of overlap between maps of cortical thinning in children treated for medulloblastoma (outlined in white) and maps of age-dependent cortical thinning. Maps displayed on lateral views of average cortical surface.

## DISCUSSION

We found a nonuniform pattern of cortical thinning in medulloblastoma patients compared with their age- and gender-matched controls. The relatively thinner cortex was seen in the posterior positions of the cerebral cortex, specifically the left perirolandic region and parieto-occipital lobes and the right parietal lobe, posterior superior temporal gyrus, and lateral temporal lobe. The average thickness differences, which were in the range of 0.2–0.4 mm, were not detectable visually, and thus required these analysis tools for accurate measurement. Interpreting abnormal development in children ideally requires comparison with normally developing children. As children get older, various regions of cerebral cortex undergo thinning at different ages, which presumably represents neuronal pruning and development (35–38). All the areas of cortical thinning seen in our study group overlapped with the regions of thinning seen in the larger control group of children.

Furthermore, the areas of relative thinning were all found in the posterior portion of the brain. This part of the brain is known to undergo age-related thinning at an earlier age (38), closely corresponding to the age at treatment of these patients. This spatial overlap between the thinner cortex in children treated for medulloblastoma and the regions of normal age-related thinning cortex suggests that the areas of cortex that are undergoing development are more sensitive to the effects of treatment of medulloblastoma. Recent imaging studies on normal children have linked cortical thickness in normal children with IQ (39, 40). Most of the cortical thinning was seen bilaterally in the parietal cortex. The parietal cortex is classically thought of as an association area, taking inputs from multiple sensory areas and projecting to multiple higher cortical areas. Recent neuroimaging data have also revealed that the parietal cortex plays a role in memory and attention (41, 42). It is also possible that dysfunction in the parietal cortex could explain many of the

neurocognitive deficits seen in children treated for medulloblastoma.

We did not find significant cortical thinning in the regions receiving the highest radiation dose. With full posterior fossa boost volumes, the greatest dose to the cerebrum occurs in the ventral temporal lobes. However, it could be that the sensitivity of the brain does not primarily depend on the radiation dose. We have postulated that the primary determinant of treatment sensitivity is the spatial and temporal pattern of normal cortical development, which places those brain regions at particular risk.

Other studies using different methods have also found abnormalities in the brains of children treated for medulloblastoma. Diffusion tensor imaging has been used to measure fractional anisotropy in white matter (14–17, 43). Compared with normal children, children treated for medulloblastoma had a decreased fractional anisotropy in multiple white matter regions (14, 15, 43). Decreases in fractional anisotropy also correlated with the craniospinal radiation dose (16) and IQ (17, 43).

Other brain structures have also been found to develop abnormally in children treated for medulloblastoma. Researchers at St. Jude Children's Research Hospital used a single mid-sagittal slice from a $T_1$-weighted MRI scan on children to examine the corpus callosum (18). The corpus callosum was automatically segmented and manually classified into seven subregions. All subregions showed a decreasing area with time, where normally one would expect an increase in area with time (44, 45). This group also manually traced the hippocampus on MRI scans from children with medulloblastoma (19). For the first 2–3 years after diagnosis, decreases in hippocampal volume were seen bilaterally. After that time, the hippocampal volumes resumed the typical normal growth pattern and began to increase with time (46–48).

In addition to these structural abnormalities, the radiation dose to different portions of the brain has been correlated with IQ. Researchers at St. Jude Children's Research Hospital examined the radiation dose to various brain compartments in children treated for ependymoma (49) and medulloblastoma, primitive neuroectodermal tumors, and atypical teratoid rhabdoid tumors (50). In the children treated for ependymoma, which involved conformal radiotherapy only, an increased radiation dose to supratentorial brain correlated significantly with a lower IQ. In the cohort of children treated for medulloblastoma, primitive neuroectodermal tumors, and atypical teratoid rhabdoid tumors, radiotherapy included craniospinal irradiation. For those children, an increased radiation dose to all brain compartments correlated with a decreasing IQ. The dose to the supratentorial compartment had the largest effect on IQ.

Our studies of the differential spatial sensitivity of the brain to irradiation will increase our understanding of the basis of radiation-induced neurocognitive damage. In addition, this information has clinical applications. The spatial maps could be used to define portions of the cortex as

avoidance structures for the purposes of radiotherapy planning, especially in situations in which the entire brain is not the target volume. This would allow us to optimize radiotherapy planning to treat the target volume and minimize the dose to the sensitive cortex. Furthermore, our explicit representation of the cortex would allow us to measure more precise dose–volume histograms and quantify the effect of dose on the neurocognitive outcomes, similar to the work from St. Jude Children's Research Hospital.

The limitations of this work primarily reflect the small number of patients and the limited number of longitudinal studies in the case subjects. The accurate measurement of the cerebral cortex, which is only a few millimeters thick,

requires high-resolution MRI, which is not typically acquired in most clinical situations. As a result, we were unable to examine many variables, including age at diagnosis, time elapsed from treatment, neuropsychological test results, and other clinical factors. However, the sensitive measurements we have described provide an important development in our understanding of the effects of radiotherapy on the brain. These results allowed us to generate a testable hypothesis, specifically that the treatment sensitivity of the brain of children treated for medulloblastoma depends on the age of the child and the normal developmental pattern of cortex. Future work with additional subjects will attempt to address these limitations.

# REFERENCES

1. Mulhern RK, Palmer SL, Merchant TE, *et al.* Neurocognitive consequences of risk-adapted therapy for childhood medulloblastoma: Attention and memory functioning among pediatric patients with medulloblastoma. *J Clin Oncol* 2005;23:5511–5519.

2. Palmer SL, Goloubeva O, Reddick WE, *et al.* Patterns of intellectual development among survivors of pediatric medulloblastoma: A longitudinal analysis. *J Clin Oncol* 2001;19:2302–2308.

3. Ris MD, Packer R, Goldwein J, *et al.* Intellectual outcome after reduced-dose radiation therapy plus adjuvant chemotherapy for medulloblastoma: A Children's Cancer Group study. *J Clin Oncol* 2001;19:3470–3476.

4. Kieffer-Renaux V, Bulteau C, Grill J, *et al.* Patterns of neuropsychological deficits in children with medulloblastoma according to craniospatial irradiation doses. *Dev Med Child Neurol* 2000;42:741–745.

5. Grill J, Renaux VK, Bulteau C, *et al.* Long-term intellectual outcome in children with posterior fossa tumors according to radiation doses and volumes. *Int J Radiat Oncol Biol Phys* 1999;45:137–145.

6. Mulhern RK, Kepner JL, Thomas PR, *et al.* Neuropsychologic functioning of survivors of childhood medulloblastoma randomized to receive conventional or reduced-dose craniospinal irradiation: A Pediatric Oncology Group study. *J Clin Oncol* 1998;16:1723–1728.

7. Yang TF, Wong TT, Cheng LY, *et al.* Neuropsychological sequelae after treatment for medulloblastoma in childhood—The Taiwan experience. *Childs Nerv Syst* 1997;13:77–80.

8. Dennis M, Spiegler BJ, Hetherington CR, *et al.* Neuropsychological sequelae of the treatment of children with medulloblastoma. *J Neurooncol* 1996;29:91–101.

9. Radcliffe J, Bunin GR, Sutton LN, *et al.* Cognitive deficits in long-term survivors of childhood medulloblastoma and other noncortical tumors: Age-dependent effects of whole brain radiation. *Int J Dev Neurosci* 1994;12:327–334.

10. Riva D, Milani N, Pantaleoni C, *et al.* Combined treatment modality for medulloblastoma in childhood: Effects on neuropsychological functioning. *Neuropediatrics* 1991;22:36–42.

11. Maddrey AM, Bergeron JA, Lombardo ER, *et al.* Neuropsychological performance and quality of life of 10 year survivors of childhood medulloblastoma. *J Neurooncol* 2005;72:245–253.

12. Seaver E, Geyer R, Sulzbacher S, *et al.* Psychosocial adjustment in long-term survivors of childhood medulloblastoma and ependymoma treated with craniospinal irradiation. *Pediatr Neurosurg* 1994;20:248–253.

13. Riva D, Pantaleoni C, Milani N, *et al.* Impairment of neuropsychological functions in children with medulloblastomas

and astrocytomas in the posterior fossa. *Childs Nerv Syst* 1989;5:107–110.

14. Khong PL, Kwong DL, Chan GC, *et al.* Diffusion-tensor imaging for the detection and quantification of treatment-induced white matter injury in children with medulloblastoma: A pilot study. *AJNR Am J Neuroradiol* 2003;24:734–740.

15. Leung LH, Ooi GC, Kwong DL, *et al.* White-matter diffusion anisotropy after chemo-irradiation: A statistical parametric mapping study and histogram analysis. *Neuroimage* 2004;21:261–268.

16. Khong PL, Leung LH, Chan GC, *et al.* White matter anisotropy in childhood medulloblastoma survivors: Association with neurotoxicity risk factors. *Radiology* 2005;236:647–652.

17. Khong P-L, Leung LHT, Fung ASM, *et al.* White matter anisotropy in post-treatment childhood cancer survivors: Preliminary evidence of association with neurocognitive function. *J Clin Oncol* 2006;24:884–890.

18. Palmer SL, Reddick WE, Glass JO, *et al.* Decline in corpus callosum volume among pediatric patients with medulloblastoma: Longitudinal MR imaging study. *AJNR Am J Neuroradiol* 2002;23:1088–1094.

19. Nagel BJ, Palmer SL, Reddick WE, *et al.* Abnormal hippocampal development in children with medulloblastoma treated with risk-adapted irradiation. *AJNR Am J Neuroradiol* 2004;25:1575–1582.

20. Fouladi M, Chintagumpala M, Laningham FH, *et al.* White matter lesions detected by magnetic resonance imaging after radiotherapy and high-dose chemotherapy in children with medulloblastoma or primitive neuroectodermal tumor. *J Clin Oncol* 2004;22:4551–4560.

21. Reddick WE, Glass JO, Palmer SL, *et al.* Atypical white matter volume development in children following craniospinal irradiation. *Neurooncology* 2005;7:12–19.

22. Reddick WE, White HA, Glass JO, *et al.* Developmental model relating white matter volume to neurocognitive deficits in pediatric brain tumor survivors. *Cancer* 2003;97:2512–2519.

23. Mulhern RK, Palmer SL, Reddick WE, *et al.* Risks of young age for selected neurocognitive deficits in medulloblastoma are associated with white matter loss. *J Clin Oncol* 2001;19:472–479.

24. Reddick WE, Russell JM, Glass JO, *et al.* Subtle white matter volume differences in children treated for medulloblastoma with conventional or reduced dose craniospinal irradiation. *Magn Reson Imaging* 2000;18:787–793.

25. Mulhern RK, Reddick WE, Palmer SL, *et al.* Neurocognitive deficits in medulloblastoma survivors and white matter loss. *Ann Neurol* 1999;46:834–841.

26. Reddick WE, Mulhern RK, Elkin TD, *et al.* A hybrid neural network analysis of subtle brain volume differences in chil-

dren surviving brain tumors. *Magn Reson Imaging* 1998;16:413–421.

27. Fischl B, Dale AM. Measuring the thickness of the human cerebral cortex from magnetic resonance images. *Proc Natl Acad Sci USA* 2000;97:11050–11055.

28. Evans AC. The NIH MRI study of normal brain development. *Neuroimage* 2006;30:184–202.

29. Sereno MI, Dale AM, Reppas JB, *et al.* Borders of multiple visual areas in humans revealed by functional magnetic resonance imaging. *Science* 1995;268:889–893.

30. Dale AM, Fischl B, Sereno MI. Cortical surface-based analysis I: Segmentation and surface reconstruction. *Neuroimage* 1999;9:179–194.

31. Fischl B, Sereno MI, Dale AM. Cortical surface-based analysis II: Inflation, flattening, and a surface-based coordinate system. *Neuroimage* 1999;9:195–207.

32. Fischl B, Liu A, Dale AM. Automated manifold surgery: Constructing geometrically accurate and topologically correct models of the human cerebral cortex. *IEEE Trans Med Imaging* 2001;20:70–80.

33. Segonne F, Dale AM, Busa E, *et al.* A hybrid approach to the skull stripping problem in MRI. *Neuroimage* 2004;22:1060–1075.

34. Rosas HD, Liu AK, Hersch S, *et al.* Regional and progressive thinning of the cortical ribbon in Huntington's disease. *Neurology* 2002;58:695–701.

35. Giedd JN, Blumenthal J, Jeffries NO, *et al.* Brain development during childhood and adolescence: A longitudinal MRI study. *Nat Neurosci* 1999;2:861–863.

36. Sowell ER, Trauner DA, Gamst A, *et al.* Development of cortical and subcortical brain structures in childhood and adolescence: A structural MRI study. *Dev Med Child Neurol* 2002;44:4–16.

37. Sowell ER, Peterson BS, Thompson PM, *et al.* Mapping cortical change across the human life span. *Nat Neurosci* 2003;6:309–315.

38. Sowell ER, Thompson PM, Leonard CM, *et al.* Longitudinal mapping of cortical thickness and brain growth in normal children. *J Neurosci* 2004;24:8223–8231.

39. Shaw P, Greenstein D, Lerch J, *et al.* Intellectual ability and cortical development in children and adolescents. *Nature* 2006;440:676–679.

40. Lerch JP, Worsley K, Shaw WP, *et al.* Mapping anatomical correlations across cerebral cortex (MACACC) using cortical thickness from MRI. *Neuroimage* 2006;31:993–1003.

41. Behrmann M, Geng JJ, Shomstein S. Parietal cortex and attention. *Curr Opin Neurobiol* 2004;14:212–217.

42. Culham JC, Kanwisher NG. Neuroimaging of cognitive functions in human parietal cortex. *Curr Opin Neurobiol* 2001;11:157–163.

43. Mabbott DJ, Noseworthy MD, Bouffet E, *et al.* Diffusion tensor imaging of white matter after cranial radiation in children for medulloblastoma: Correlation with IQ. *Neurooncology* 2006;8:244–252.

44. Thompson PM, Giedd JN, Woods RP, *et al.* Growth patterns in the developing brain detected by using continuum mechanical tensor maps. *Nature* 2000;404:190–193.

45. Giedd JN, Blumenthal J, Jeffries NO, *et al.* Development of the human corpus callosum during childhood and adolescence: A longitudinal MRI study. *Prog Neuropsychopharmacol Biol Psychiatry* 1999;23:571–588.

46. Pfluger T, Weil S, Weis S, *et al.* Normative volumetric data of the developing hippocampus in children based on magnetic resonance imaging. *Epilepsia* 1999;40:414–423.

47. Utsunomiya H, Takano K, Okazaki M, *et al.* Development of the temporal lobe in infants and children: Analysis by MR-based volumetry. *AJNR Am J Neuroradiol* 1999;20:717–723.

48. Giedd JN, Vaituzis AC, Hamburger SD, *et al.* Quantitative MRI of the temporal lobe, amygdala, and hippocampus in normal human development: Ages 4–18 years. *J Comp Neurol* 1996;366:223–230.

49. Merchant TE, Kiehna EN, Li C, *et al.* Radiation dosimetry predicts IQ after conformal radiation therapy in pediatric patients with localized ependymoma. *Int J Radiat Oncol Biol Phys* 2005;63:1546–1554.

50. Merchant TE, Kiehna EN, Li C, *et al.* Modeling radiation dosimetry to predict cognitive outcomes in pediatric patients with CNS embryonal tumors including medulloblastoma. *Int J Radiat Oncol Biol Phys* 2006;65:210–221.